Cubic or monoclinic Y_2O_3:Eu nanoparticles by flame spray pyrolysis

A. Camenzind, R. Strobel and S.E. Pratsinis

Swiss Federal Institute of Technology, Particle Technology Laboratory, Institute of Process Engineering, Department of Mechanical and Process Engineering, CH-8092 Zurich, Switzerland,
camenzind@ptl.mavt.ethz.ch, www.ptl.ethz.ch

ABSTRACT

Monocrystalline cubic and/or monoclinic $Y_2O_3:Eu^{3+}$ nanoparticles (10-50 nm) were synthesized continuously without post-processing by single-step flame spray pyrolysis (FSP). These particles were characterized by X-ray diffraction (XRD), nitrogen adsorption (BET) and transmission electron microscopy (TEM). Photo-luminescence (PL) emission was measured as well as the time-resolved PL-intensity decay. Synthesis of single and mixed crystal phase (monoclinic and/or cubic) $Y_2O_3:Eu^{3+}$ nanoparticles was achieved by controlling the precursor combustion conditions in the flame, hence the temperature profile (maximum flame temperature, cooling rate) as well as high temperature residence time which resulted in different particle growth histories which in turn affected particle characteristics as crystal phase, size and morphology. Longer high temperature residence time of the particles resulted in cubic nanoparticles with lower maximum PL-intensity than measured by commercial micron-sized bulk $Y_2O_3:Eu^{3+}$ phosphor powder.

Keywords: flame spray pyrolysis, $Y_2O_3:Eu^{3+}$, nanophosphors, monoclinic, cubic

1 INTRODUCTION

Eu^{3+}-doped yttrium oxide ($Y_2O_3:Eu^{3+}$) is a red emitting phosphor commonly used in lightning and display applications [1]. Even though good knowledge of its bulk properties has been developed [1], new approaches are necessary to understand and investigate ongoing physics in nanosized phosphors. For enhanced luminescence and resolution of displays, phosphors with controlled morphology, small sizes (in the nanometer range) and good dispersion in various matrices were investigated within the last few years. Moreover, non- or weakly-agglomerated particles are required for stable slurries for manufacturing of displays [2]. Rare earth oxides showed advanced and promising properties as stability in vacuum and corrosion-free gas emission under electron bombardment in cathode ray tube applications [3]. Further more these materials have a high damage-resistance and high-reflectance in light-emitting diodes and high-power pulsed ultraviolet lasers [3]. However, few nano-phosphors based on $Y_2O_3:Eu^{3+}$ with luminescence brightness as high as commercial bulk phosphors have been reported to date [2]. Since technical applications will hardly focus on the use of single particles except in bio-chemical applications [4,5] the interactions between nanoparticles is required to be investigated in more detail. In the last years several studies investigated nanosized $Y_2O_3:Eu^{3+}$ particles towards their physical, electronic and optical property changes compared to bulk materials [6,7]. Optical properties as the shift of the charge-transfer band, phonon relaxation and spontaneous transition rates were reported to vary when the particle size is reduced to the nanoscaled [8]. The higher surface-to-volume ratio of nanoparticles and increased defects at the surface were suggested to result in quenched luminescence [9].

Nanosized europium-doped yttria has been synthesized via different preparation routes. The sol-gel process [10] and microemulsion method (ME) [11] were introduced in the field of wet chemistry and alternative routes as combustion synthesis (CS) [12] which all have shown the capability to produce nanosized structures. Lately, new approaches were introduced to meet the today's need for nanosized phosphors. Especially in the gas phase many approaches have been undertaken as for example laser ablation [13] and spray pyrolysis (SP) in tubular, hot-wall [2,6,7,14] or vapor flame-supported [15,16] reactors (VFSP). The use of spray pyrolysis in tubular, hot-wall reactors has a major weakness as it results often in micrometer sized hollow particles with porous structures [14]. Another frequently used technique is spray pyrolysis in flame-supported reactors, where droplets of yttrium/europium nitrate dissolved in water [15,16] are formed by a nebulizer and brought into a methane-oxygen diffusion flame where the phosphor is formed. Following the notation of Mädler [17] this method is called vapor-flame-supported spray pyrolysis (VFSP). Particles synthesized with this method were either hollow, shell-like products or inhomogeneous particles with nanosized, hairy structures at their surface (broad size distribution) [15,16].

Flame spray pyrolysis (FSP) combined with the advantages of an appropriate, organometallic precursor [18] was used to synthesis $Y_2O_3:Eu^{3+}$ nanoparticles of controlled size and crystallinity. Yttrium and europium was dissolved in a liquid, combustible, organometallic precursor solution which was dispersed with a high velocity oxygen gas stream fed into a nozzle. The formed droplet spray was ignited by a supporting methane flame as reported in more detail elsewhere [19]. Altering the flame condition via the liquid precursor flow rate and dispersion gas flow rate

allowed varying combustion conditions, flame height as well as gas velocities [18]. Consequently, the high temperature residence time of particles in the flame as well as flame temperature profile of the flame were strongly affected. However, changing the flame conditions allowed studying the particle growth and consequent particle morphology changes.

2 EXPERIMENTAL

2.1 Particle Synthesis

The precursor consisted of Eu(III)2-ethylhexanoate (Strem Chemicals, 99.9%) and yttrium(III)2-ethylhexanoate solution (dissolved in 2-ethylhexanoic acid: 0.8 M) which was prepared via converting Y(III)-nitrate-hexahydrate (Aldrich, 99.9%) to $Y(OH)_3$ (with aqueous ammonia and subsequent washing with destilled water) and further processing with 2-ethylhexanoic acid and acetic anhydride (both Riedel-de Haën, 99%) (refluxing at 65°C for 4 hours [20]). The appropriate amounts of Eu(III)2-ethylhexanoate and Y(III)2-ethylhexanoate were dissolved in toluene to form the final precursor with a total metal concentration of 0.4 M.

The flame spray setup used in this study (described in more detail elsewhere [19]) as well as the above presented preparation of the precursors was equal to the one used in the previous work [18]. A syringe pump (Inotech) maintained a constant feed rate of the precursor mixture into a small capillary. At the capillary tip the precursor solution was dispersed by an oxygen jet formed around the capillary by the surrounding nozzle with a pressure drop of 1.5 bar [19]. The precursor feed rate was varied between 5-8 ml/min and the oxygen flow rate between 3-5 l/min. Supporting flamelets (positioned in a ring around the nozzle outlet) fed with oxygen (2.4 l/min) and methane (1.13 l/min) assisted the evaporation of the liquid precursor droplets and the final precursor combustion [19]. In the flame nanosized Y_2O_3:Eu^{3+} particles were formed by nucleation, condensation, coagulation and agglomeration processes [17,21] and collected on a glass microfibre filter (GF/A Whatman, 257 mm in diameter) by the aid of a vacuum pump (Busch, Seco SV 1040C).

The as-prepared materials were designated as YαEu-β/γ, where α depicts the mass fraction of europium (wt%), β stands for the precursor feed rate in ml/min and γ for the oxygen dispersion gas flow rate in l/min. The europium content of flame made Y_2O_3:Eu^{3+} was altered from 0 to 7 wt%. For comparison a commercial, bulk Y_2O_3:Eu^{3+} phosphor was used.

2.2 Characterization

The specific surface area (SSA) was determined according to Brunauer-Emmett-Teller (BET) at -196 °C (Micromeritics Tristar). The samples were outgassed at 150 °C for 1 hour prior to analysis. The BET corresponding particle diameters were calculated accounting for the mass fraction of each Y_2O_3 crystal phase (monoclinic and cubic) and the corresponding densities (Y_2O_3-monoclinic: 5.5 g/cm^3, Y_2O_3-cubic: 5.01 g/cm^3, Eu_2O_3: 7.42 g/cm^3). X-ray diffraction (XRD) patterns were recorded with a Bruker D8 advance diffractometer (40 kV, 40 mA, CuKα) at 2θ = 20-80 ° with a step size of 0.06 ° and a scan speed of 0.72 °/min. With the fundamental parameter approach and Rietveld refining method [22,23] the phase mass fraction and the corresponding monoclinic or cubic crystal sizes were calculated using the software TOPAS. The structural parameters of cubic yttria (Inorganic Crystal Structure Database [ICSD] Coll. Code: 26190 [24]) and monoclinic yttria (modified structural parameters of ICSD Coll. Code.: 84125 [25]) were applied. TEM analysis was performed on a Tecnai 30F microscope (Philips; Field emission cathode, operated at 300 kV). TEM images were recorded on a slow-scan CCD camera.

The emission spectra were recorded at room temperature using a fluorescence spectrophotometer (Varian Cary Eclipse) with a spectral resolution of 0.25 nm. Samples of 100 mg each were filled into a cylindrical powder holder (10 mm in diameter) and exposed to UV photons supplied by a flash xenon lamp (80 flashes/s). The emission spectra (excitation at 254 ±2.5 nm) were measured in the range of 570 nm to 640 nm at a scan speed of 167 nm/min.

3 RESULTS

Flame spray pyrolysis of Y_2O_3:Eu^{3+} resulted in crystalline nanoparticles as shown in the previous work [18]. Figure 1 shows HR-TEM images of these Y_2O_3:Eu^{3+} particles made at different flame conditions. A relatively low enthalpy content and short flame (Y5Eu-5/5: 33.4 kJ/$l_{disp.gas}$ derived from the ratio of liquid precursor enthalpy feed rate [kJ/min] divided by the dispersion gas flow rate [$l_{disp.gas}$/min] [18]) formed spherical particles with an approximate size of 10 nm (Fig. 1a), whereas increased flame enthalpy and longer flames (Y5Eu-8/3: 89.1 kJ/$l_{disp.gas}$) led to larger particles with a rhombohedral shape (Fig. 1a and b).

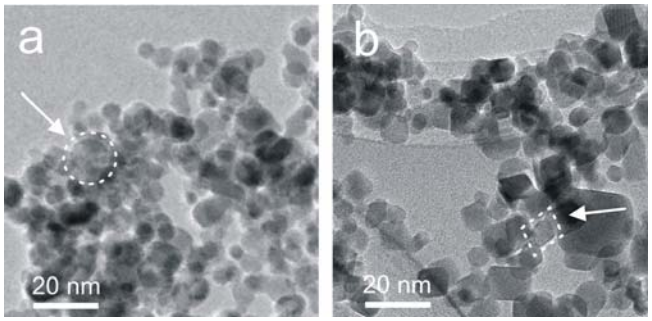

Figure 1 HR-TEM images of flame-made Y_2O_3:Eu^{3+} nanoparticles made in a) low (YEu-5/5) and b) high (YEu-8/3) enthalpy flames [18].

Figure 2 shows the BET corresponding particle diameter (open diamonds), phase composition (cubic/monoclinic: diamonds) and crystal sizes corresponding to the monoclinic (open triangles) or cubic crystal phase (open squares) of these flame-made Y_2O_3:Eu^{3+} particles according to detailed XRD analysis using the fundamental parameter approach and Rietveld refining method [22,23]. The BET corresponding particle diameter increased from 11 nm to 23 nm with increasing specific combustion enthalpy. The average crystal size was calculated from the monoclinic and cubic crystal sizes as well as accounting for the cubic/monoclinic phase composition, both extracted from the XRD pattern (using the above mentioned method [22,23]). The mass weighted averaged crystal sizes (open circles) were slightly larger than the BET diameter and the size difference (BET to XRD) is more distinct in case of the Y5Eu-8/3 than compared to the Y5Eu-5/5 particles. Smaller flames (11 cm: lower specific combustion enthalpies) led to smaller, mainly monoclinic particles, whereas longer flames (24 cm: higher specific combustion enthalpies) resulted in the formation of larger particles with pronounced cubic crystal structure.

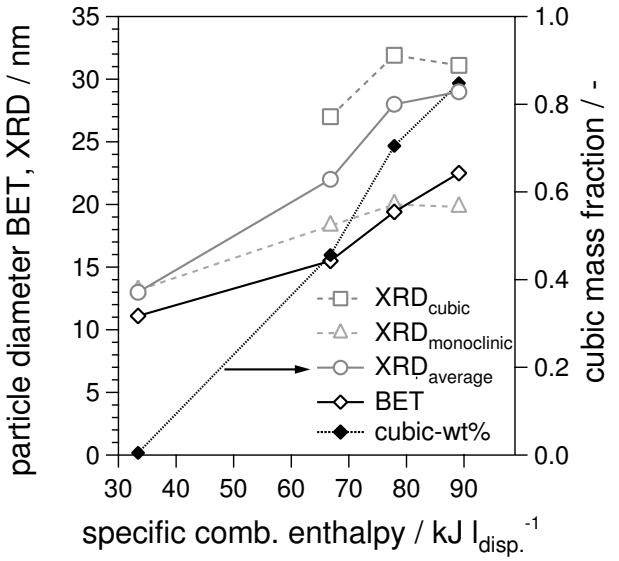

Figure 2 BET equivalent diameter [nm] (open diamonds), cubic (open squares) and monoclinic crystal size (XRD: open triangles) and averaged crystal size (open circles) by taking the mass fraction of the monoclinic and cubic crystal phase (second axis: diamonds) into account as a function of the specific combustion enthalpy (liquid precursor enthalpy feed rate [kJ/min] divided by the dispersion gas flow rate [$l_{disp.gas}$/min]).

The influence of europium content on photoluminescent properties was investigated with particles of different Eu contents, synthesized in the longest flame (YαEu-8/3). Figure 3 shows the maximum photoluminescence (PL) intensity emission peak (at 612 nm) of these phosphors and the cubic mass fraction determined by XRD. The BET corresponding particle size varied not significantly (d_{BET} = 23±1nm, $d_{XRD,cubic}$ = 34±2nm, $d_{XRD,monoclinic}$ = 22±1nm). The as-prepared particles showed all nearly cubic crystal structure but the maximum PL intensity varied with Eu content and a concentration of 5wt% (3.8 mol%) was an optimum since higher doped particles showed no increased PL emission intensity.

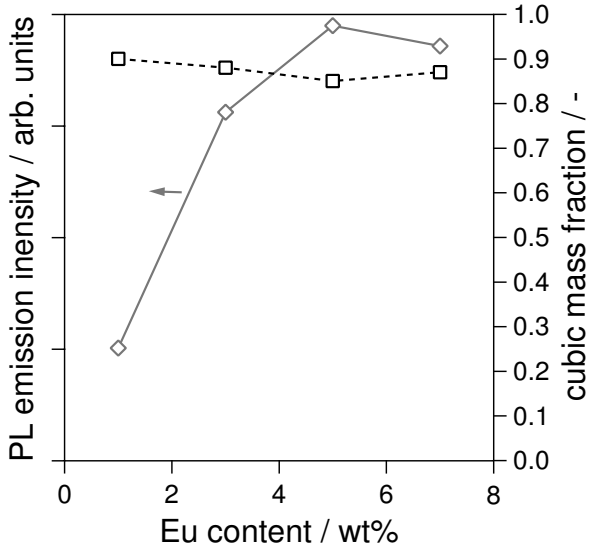

Figure 3 Maximum photoluminescence emission intensity measured at 612 nm (open diamonds) of flame made nanoparticles (YαEu-8/3) with varying Eu content (1-7 wt%) with the corresponding cubic mass fraction (second axis: open squares).

4 DISCUSSION

Most previous studies using the concept of spray pyrolysis often used aqueous metal nitrate solutions resulting in rather inhomogeneous particles [6,15,16], large particles [2] or small agglomerated particles [7]. The inhomogeneity is attributed to the inadequate choice of precursor [26,27]. Here and also as it was presented in an earlier study [18], an appropriate organometallic precursor led to the formation of nanosized, homogeneous particles [20]. The formation of either monoclinic or cubic Y_2O_3:Eu^{3+} nanoparticles could be controlled by altering the flame conditions [18]. The precursor feed rate and the dispersion gas flow rate determine the enthalpy density in the flame and affect the temperature profile and the metal concentration, which then contributes to the nucleation and coagulation rates [28]. Longer flames with increased residence time of the particles at high temperatures were formed with higher specific combustion enthalpies (Y5Eu-8/3,-7/3,-6/3). The close control of temperature profile and residence time of particles in the hot flame allowed forming tailor-made nanoparticles. Longer particle residence time formed

partially monoclinic but mainly cubic, rhombohedrally shaped particles (Y5Eu-8/3: Fig. 1a and b) and short flames with particles rapidly passing the hot region shaped spherical, monoclinic particles (Y5Eu-5/5: Fig. 1a). The evolution of the crystal phase composition from monoclinic to cubic and particle growth with elongated flames was observed (Fig. 2). The small divergence of particle size with elongated flames considering XRD and BET measurements (Fig. 2) is attributed to the rhombohedral shape of the cubic particles.

When the concentration of luminescent centers (here Eu^{3+}) is increased, energy from one centre can migrate to another since the atomic distance to each other is reduced. The probability for non-radiative decay increases and this effect is known as the concentration quenching effect in phosphor materials [1]. Some contrary results were found over the last few years. In bulk materials the concentration quenching starts at 6-8 mol% Eu^{3+} [12], however sub micron-sized particles showed the concentration quenching effect at 10-18 mol% [12]. It was suggested that the particle size (determined by either XRD or TEM) had a major impact onto the concentration quenching, since they found higher quenching concentrations with smaller particle sizes. Here (Fig. 3), the concentration quenching effect of approximately equally sized YαEu-8/3 particles (23±1 nm by BET) was observed at 5 wt% Eu (3.8 mol%).

5 CONCLUSION

Flame spray pyrolysis (FSP) combined with the advantages of an appropriate, organometallic precursor was used for synthesis of solid Y_2O_3:Eu^{3+} nanoparticles (< 30 nm) of controlled size and crystallinity without post-processing. Adjustment of FSP-process parameters allowed controlling the high temperature particles residence time and hence particle growth, morphology and crystal phase composition. The photoluminescent (PL) emission intensity and the radiative decay time showed size effects since nanosized flame-made particles had lower PL intensities than a commercial phosphor but prolonged radiative decay. The influence of Eu content on the PL emission intensity showed a concentration quenching effect for the as-prepared, non-agglomerated particles (23 nm) at 5 wt% Eu.

REFERENCES

[1] G. Blasse, B.C. Grabmaier, Luminescent Materials (Springer, Berlin, 1994).

[2] Y. Shimomura, N. Kijima, *Electrochem. Solid St.* 7, H18 (2004).

[3] K. Zhang, A.K. Pradhan, G.B. Loutts, U.N. Roy, Y.L. Cui, A. Burger, *J. Opt. Soc. Am. B* 21, 1804 (2004).

[4] P. Alivisatos, *Nat. Biotechnol.* 22, 47 (2004).

[5] C.M. Niemeyer, *Angew. Chem. Int. Edit.* 40, 4128 (2001).

[6] A. Konrad, U. Herr, R. Tidecks, F. Kummer, K. Samwer, *J. Appl. Phys.* 90, 3516 (2001).

[7] R. Schmechel, M. Kennedy, H. von Seggern, H. Winkler, M. Kolbe, R.A. Fischer, X.M. Li, A. Benker, M. Winterer, H. Hahn, *J. Appl. Phys.* 89, 1679 (2001).

[8] B.M. Tissue, H.B. Yuan, *J. Solid State Chem.* 171, 12 (2003).

[9] J. McKittrick, C.F. Bacalski, G.A. Hirata, K.M. Hubbard, S.G. Pattillo, K.V. Salazar, M. Trkula, *J. Am. Ceram. Soc.* 83, 1241 (2000).

[10] P.K. Sharma, R. Nass, H. Schmidt, *Opt. Mater.* 10, 161 (1998).

[11] H. Huang, G.Q. Xu, W.S. Chin, L.M. Gan, C.H. Chew, *Nanotechnology* 13, 318 (2002).

[12] W.W. Zhang, W.P. Zhang, P.B. Xie, M. Yin, H.T. Chen, L. Jing, Y.S. Zhang, L.R. Lou, S.D. Xia, *J. Colloid Interf. Sci.* 262, 588 (2003).

[13] H. Eilers, B.M. Tissue, *Chem. Phys. Lett.* 251, 74 (1996).

[14] K.Y. Jung, K.H. Han, *Electrochem. Solid St.* 8, H17 (2005).

[15] Y.C. Kang, D.J. Seo, S.B. Park, H.D. Park, *Jpn. J. Appl. Phys.* 40, 4083 (2001).

[16] H. Chang, I.W. Lenggoro, K. Okuyama, T.O. Kim, *Jpn. J. Appl. Phys.* 43, 3535 (2004).

[17] L. Mädler, *KONA Powder and Particle* 22, 107 (2004).

[18] A. Camenzind, R. Strobel, S.E. Pratsinis, *Chem. Phys. Lett.* 415, 193 (2005).

[19] L. Mädler, W.J. Stark, S.E. Pratsinis, *J. Mater. Res.* 17, 1356 (2002).

[20] R. Jossen, R. Mueller, S.E. Pratsinis, M. Watson, M.K. Akhtar, *Nanotechnology* 16, (2005).

[21] S.E. Pratsinis, *Prog. Energ. Combust.* 24, 197 (1998).

[22] H.M. Rietveld, *J. Appl. Crystallogr.* 2, 65 (1969).

[23] R.W. Cheary, A.A. Coelho, *J. Appl. Crystallogr.* 31, 851 (1998).

[24] B.H. O'Connor, T.M. Valentine, *Acta Crystallogr.* B25, 2140 (1969).

[25] B. Antic, M. Mitric, D. Rodic, *J. Phys.-Condens. Mat.* 9, 365 (1997).

[26] R. Jossen, S.E. Pratsinis, W.J. Stark, L. Madler, *J. Am. Ceram. Soc.* 88, 1388 (2005).

[27] L. Mädler, S.E. Pratsinis, *J. Am. Ceram. Soc.* 85, 1713 (2002).

[28] S.E. Pratsinis, W.H. Zhu, S. Vemury, *Powder Technol.* 86, 87 (1996).